

# Organic & Biomolecular Chemistry

Accepted Manuscript



This is an *Accepted Manuscript*, which has been through the Royal Society of Chemistry peer review process and has been accepted for publication.

*Accepted Manuscripts* are published online shortly after acceptance, before technical editing, formatting and proof reading. Using this free service, authors can make their results available to the community, in citable form, before we publish the edited article. We will replace this *Accepted Manuscript* with the edited and formatted *Advance Article* as soon as it is available.

You can find more information about *Accepted Manuscripts* in the [Information for Authors](#).

Please note that technical editing may introduce minor changes to the text and/or graphics, which may alter content. The journal's standard [Terms & Conditions](#) and the [Ethical guidelines](#) still apply. In no event shall the Royal Society of Chemistry be held responsible for any errors or omissions in this *Accepted Manuscript* or any consequences arising from the use of any information it contains.

## Design and synthesis of a new dimeric xanthone derivative: enhancement of G-quadruplex selectivity and telomere damage.

Marco Franceschin(1)\*, Daniele Nocioni(1), Annamaria Biroccio(2), Emanuela Micheli(3,4), Stefano Cacchione(3,4), Chiara Cingolani(2), Alessandro Venditti (1), Pasquale Zizza(2), Armandodoriano Bianco(1), Alessandro Altieri(1)\*

1) University of Rome "Sapienza", Department of Chemistry, Piazzale Aldo Moro 5, Roma 00185, Italy

2) Experimental Chemotherapy Laboratory, Regina Elena National Cancer Institute;

3) University of Rome "Sapienza", Department of Biology and Biotechnology "Charles Darwin", Piazzale Aldo Moro 5, Roma 00185, Italy

4) Istituto Pasteur-Fondazione Cenci-Bolognetti, Piazzale Aldo Moro 5, Roma 00185, Italy

\*correspondence should be addressed to [alessandro.altieri@uniroma1.it](mailto:alessandro.altieri@uniroma1.it) and [marco.franceschin@uniroma1.it](mailto:marco.franceschin@uniroma1.it)

**Keywords:** G-quadruplex; xanthene; xanthone; ESI-MS; FRET; telomere; c-myc; bcl-2

**Abstract:** Following the results we previously reported on a series of xanthene and xanthone derivatives as G-quadruplex stabilizing ligands, in order to obtain a more selective compound with respect to the previous generation of derivatives, we decided to modify the structure of the core ligand, specifically its aromatic extension. In particular, here we report the design, synthesis and activity data of a new compound, obtained by dimerization of the xanthene core (HELIXA4C). The reported results show that the extension of the aromatic core and the increasing of the number of polar side chains led to great enhancement of G-quadruplex selectivity and telomere damage capability, as derived by ESI-MS evaluation, *in vitro* cancer screening and specific immunofluorescence assays.

## Introduction

The G-quadruplex, stabilized by Hoogsteen hydrogen bonds, is one of the most important secondary structures of nucleic acids, which forms in G-rich sequences under some monovalent cations<sup>1</sup>. These special secondary structures are present in important regions of the eukaryotic genome, such as telomeres and the regulatory regions of several genes; therefore such structures play important roles in the regulation of biological events<sup>2,3,4,5</sup>. In recent years, the G-quadruplex has attracted intense interest because of its potential biological functions, such as gene regulation, gene expression and antitumor potential<sup>6</sup>. Notably, G-rich sequences are unevenly distributed on some regions of the human genome, including telomeric ends, immunoglobulin switch regions and regulatory elements in some oncogene promoters, such as c-

myc, bcl2, and others<sup>7,8,9</sup>. During these decades, different studies indicated that formation of G-quadruplexes in these regions may play important regulatory roles. Therefore, the G-quadruplex is considered a promising target for antitumor drug design<sup>10</sup>.

Following the results we previously reported on a series of xanthene and xanthone derivatives as G-quadruplex stabilizing ligands<sup>11</sup>, in order to obtain a more selective compound with respect to the previous generation of derivatives, we decided to modify the structure of the core ligand, specifically its aromatic extension (Figure 1). In particular, here we report the design, synthesis, the activity data and a docking clarification of the binding mode of a new compound, obtained by dimerization of the xanthene core (HELIXA4C). In fact, we expect that expanding the aromatic core selectivity towards G-quadruplex structures should increase with respect to duplex DNA, as for instance previously shown for coronene derivatives<sup>12</sup>.

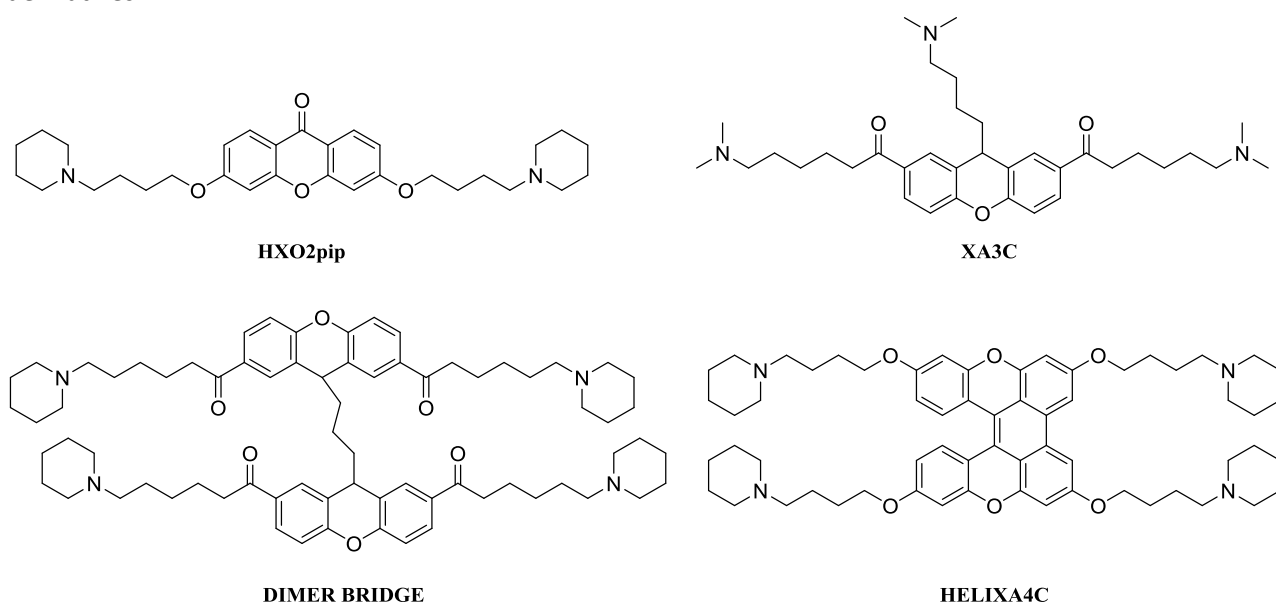


Figure 1 Chemical structures of selective previously synthesized xanthene and xanthone derivatives ligands and the new proposed ligand (HELIXA4C).

## Results and discussion

### Chemistry

We reached our synthetic target, using a variant of the McMurry reaction<sup>13</sup>. It is an organic reaction in which two ketone groups are coupled to an alkene using titanium chloride (TiCl<sub>4</sub>) and a reducing agent<sup>14,15</sup>. By this way, we obtained in a single step the dimerization and also the double bond required for the planar structure (Figure 2

Figure 2 a) Cl(CH<sub>2</sub>)<sub>4</sub>Cl (6eq), K<sub>2</sub>CO<sub>3</sub>, DMF, 70°C, 7h. 73%. b) Zn, AlCl<sub>3</sub>, THF, Microwave 12W, 60°C, 10min. 80%. c) hν, I<sub>2</sub>, THF 7h. 80% d) Piperidine (8eq), ACN, reflux. 4h. 60%). We improved the protocol changing the conditions and reagents used. The best yields were obtained when the reaction was performed in the presence of AlCl<sub>3</sub> as Lewis acid, in place of TiCl<sub>4</sub>. We observed that the protocol would be improved if the reaction is carried out by microwaves. Only 10 minutes irradiation, at 12W power and 60°C, are required to obtain the product with yields higher than 80%. The crude product, unlike the previous attempts with other Lewis acids, can be easily extracted in the organic phase. By subsequent purification, we obtained it as a pure yellow crystalline solid.

As for the opportunity to further extend the aromatic core, obtaining a more planar structure, we used a protocol already known that implies the dissolution of the sample in chloroform in presence of UV light and air<sup>16,17</sup>, with the variation to add argon to avoid the presence of oxygen, using iodine as oxidizing agent<sup>18,19</sup>, in order to avoid oxidation back to xanthone. We also varied the reaction time, the solvent in which the compound was dissolved and the power of the lamp in which the sample was exposed (12 lamp x 12W or one x 500W). In all these cases the main product obtained was the one in which one of the two possible additional cycles was closed, called helixanthen **4**. This compound was sufficiently stable under normal physiological conditions: NMR analysis of the compound, dissolved in water and kept in the sun light, were repeated after 20 days on the same sample. The spectra were the identical and this confirmed its stability. The chlorine atom was then substituted with the secondary amine and finally after the subsequent formation of the relative hydrochloride, we obtained a yellow-orange solid (HELIXA4C).

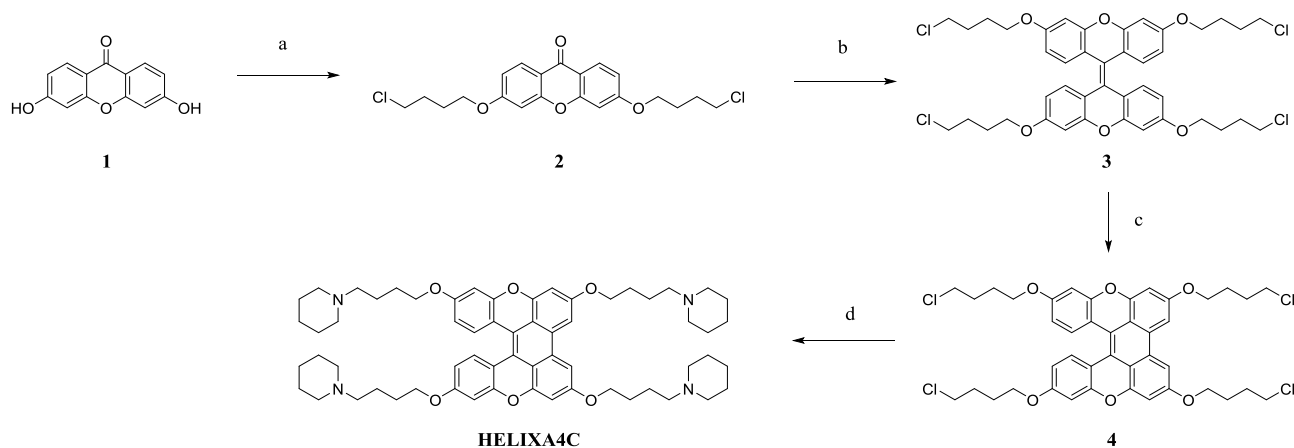


**Figure 2** a)  $\text{Cl}(\text{CH}_2)_4\text{Cl}$  (6eq),  $\text{K}_2\text{CO}_3$ , DMF,  $70^\circ\text{C}$ , 7h. 73%. b) Zn,  $\text{AlCl}_3$ , THF, Microwave 12W,  $60^\circ\text{C}$ , 10min. 80%. c) hv,  $\text{I}_2$  THF 7h. 80% d) Piperidine (8eq), ACN, reflux. 4h. 60%.

### Docking calculation

In order to clarify the mode of binding of the new compound, here we have adopted a docking approach available in the AutoDock suite of programs. This is a software suite for predicting the optimal bound conformations of ligands to macromolecules<sup>20,21,22</sup>. We obtained the initial coordinates for the docking from the Protein Data Bank coordinates of the crystal structure of the parallel 22-mer telomeric G-quadruplex (PDB ID: 1KF1) which shows a single topology, the parallel fold<sup>23,24</sup>. The corresponding intermolecular energy values were used to calculate the average binding energies (and the relative standard deviations), reported in table 1. Repeated experiments show good reproducibility, suggesting that the number of structures generated was sufficient to be statistically significant. The binding poses calculated for these compounds were then visually inspected to discard all the ligands that were not able to form hydrogen bonds with any of the guanine bases and/or to establish an electrostatic interaction with the backbone phosphate groups. Although a full planar aromatic core is expected to improve the interactions with the G-tetrad and therefore the binding to the G-quadruplex structure, we have previously shown that this also may lead to self-aggregation and reduced biological activity<sup>25</sup>. Indeed, we found that a certain degree of distortion of the aromatic core improves water solubility and selectivity for G-quadruplex over duplex DNA, as in the case of EMICORON<sup>26</sup>. For these reasons we have focused our attention on the aromatic core of HELIXA4C. In fact, despite the molecule is not fully planar, it shows a good interaction with quadruplex DNA (Figure 3).

Compound	Binding Energy
HXO2pip	-5.0
BRIDGE DIMER	-7.0
XA3C	-6.4
HELIXA 4C	-8.3

Table 1 Docking binding energies (kcal/mol) for different compounds with 1KF1. The rmsd values for the whole complex are <math><4\text{\AA}</math>.

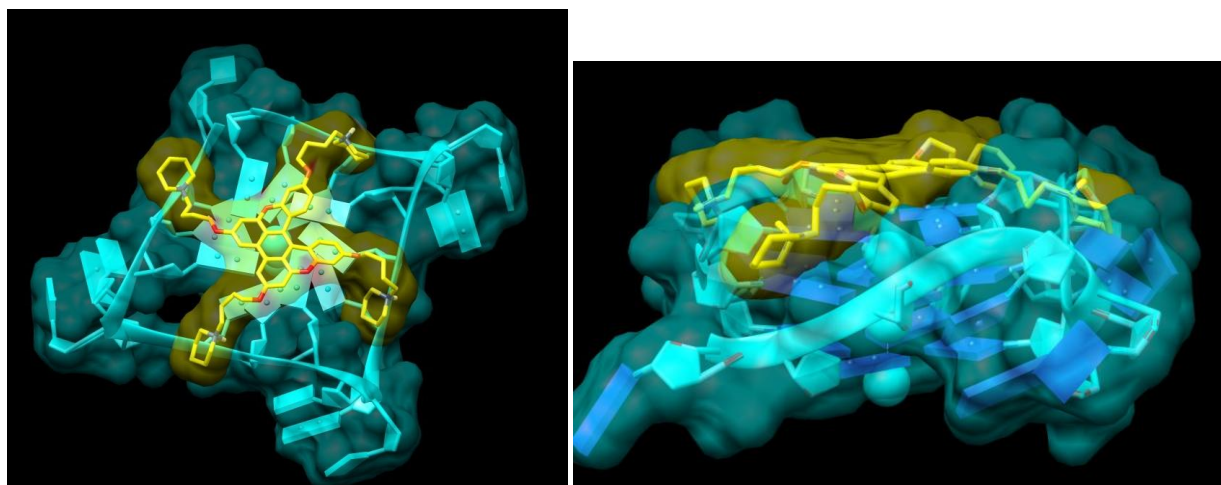


Figure 3 Model complex obtained between HELIXA4C (yellow) and the telomeric G-quadruplex DNA (blue)

### ESI-MS evaluation and G-quadruplex melting assays

As done for the previously reported compounds<sup>27,28</sup>, also in this case first of all we tested the ability of the obtained compound HELIXA4C to bind oligonucleotides in G-quadruplex conformation by ESI-MS.<sup>29,30</sup> The association constants were comparable with the best ligands tested to date among those prepared in our group, CORON and EMICORON<sup>31, 32</sup>. They were in fact also higher than those obtained for the previously reported xanthene and xanthone derivatives<sup>11</sup>. A further evidence of the ability of HELIXA4C to stabilize G-quadruplex formation come from a DNA melting assay, a straightforward method to analyze ligand binding to G-quadruplex and duplex DNA<sup>33,34</sup>. We measured the CD melting profiles of HTelo21 in presence and in absence of HELIXA4C and found that the drug increases the melting temperature of HTelo21 of 15°C ( $\Delta T_m = 15 \pm 0.4^\circ\text{C}$ ; drug/DNA = 5). Furthermore, the selectivity for G-quadruplex with respect to duplex DNA (represented by the simple dodecamer model DK66) resulted to be highly improved (Table 2).

	HTelo21				DK66		
	Log $K_1$	Log $K_2$	DNA bound 1:1	DNA bound 1:2	Log $K_1$	Log $K_2$	DNA bound 1:4
HXO2pip	4.7 ± 0.1	4.6 ± 0.1	25 ± 3	41 ± 5	3.4 ± 0.1	–	12 ± 5
Bridge Dimer	5.8 ± 0.1	5.6 ± 0.2	47 ± 2	57 ± 2	3.9 ± 0.1	3.3 ± 0.1	16 ± 2
XA3c	5.2 ± 0.4	4.9 ± 0.1	41 ± 3	50 ± 2	3.6 ± 0.3	2.9 ± 0.2	13 ± 6
HELIXA4C	6.1 ± 0.1	5.8 ± 0.2	61 ± 2	70 ± 2	3.8 ± 0.2	3.1 ± 0.2	14 ± 5

Table 2 Percentage values of DNA bound and equilibrium association constants,  $K_1$  and  $K_2$ , reported on a logarithmic scale for the complexes between the synthesized HELIXA4C and the indicated oligonucleotides as derived by ESI-MS experiments. For comparison, values relative to the most representative compounds above mentioned emerging from our previous studies are also reported.

In order to achieve a more reliable study of selectivity, we performed competition experiments on the compound HELIXA4C, in the simultaneous presence of a G-quadruplex forming oligonucleotide (specifically HTelo21 oligo) and fragments of double stranded genomic DNA (calf thymus DNA, henceforth abbreviated as CT) in 1:1 and 1:2 ratios, calculated on the basis of the phosphate group concentrations<sup>35</sup>. The analysis of the measures shows that the percentage value of quadruplex bound at a 1:1 duplex/quadruplex ratio had a poor decrease: from 61% to 55% with HTelo21, which is more than 80% left with respect to the value in the absence of CT. This result confirmed the strong preference of this molecule for the G-quadruplex structure of DNA. At a 5:1 duplex/quadruplex ratio, HELIXA4C was still able to bind 37% of the G-quadruplex DNA formed in the sample by HTelo21, which was about 2/3 of the quadruplex bound in the absence of duplex DNA (Table 3)

	Parameter	[CT] = 0	[HTelo21]:[CT] 1:1	[HTelo21]:[CT] 1:2
Xa3c	Amount bound	47.2 ± 2	41.2 ± 3	34.8 ± 3
	N	1	87.3	73.7
HELIXA4C	Amount bound	61 ± 2	55.2 ± 3	50.1 ± 3
	N	1	87.3	73.7

**Table 3** Competition experiments on HTelo21 oligo with HELIXA4C and Xa3c<sup>11</sup>. Values of percentage bound DNA as derived from Equation 7 (see experimental section) for samples containing a fixed amount of both drug and G-quadruplex DNA (5 μM, 1:1 ratio) and different amounts of calf thymus DNA (CT), at the indicated quadruplex/duplex ratios (in phosphate ions). N is the normalized percentage of bound quadruplex, defined as follows: N = (% quadruplex bound in presence of CT)/(% quadruplex bound in absence of CT).

We also decided to perform a study of the non-covalent interactions of other different G-quadruplex forming sequences with the HELIXA4C by ESIMS. We used two different oligonucleotides that could form G-quadruplex structures, taken from G-rich promoter sequences of two human oncogenes (c-myc, 5'-GAGGGTGGGGAGGGTGGGGAA-3'<sup>36</sup>, and bcl2, 5'-GGGCGCGGGAGGAAGGGGGCGGG-3'<sup>37</sup>). The results are summarized in table 4: HELIXA4C showed high percentages of DNA bound, over 50%. Nevertheless, it is evident from the association constants a lower ability to bind oncogenic sequences, in particular antiparallel bcl2, with respect to the telomeric sequence, which had a approximately 10% higher percentage of DNA bound.

These results suggest a moderate selectivity towards the topology of G-quadruplex-forming sequences. Parallel structures like telomeric DNA or c-myc are preferred to the antiparallel one (bcl2).

	bcl2				c-myc			
	LogK <sub>1</sub>	LogK <sub>2</sub>	DNA bound 1:1	DNA bound 1:2	LogK <sub>1</sub>	LogK <sub>2</sub>	DNA bound 1:1	DNA bound 1:2
XO2pip	2.0 ± 0.3	1.6 ± 0.2	5 ± 2	15 ± 5	2.2 ± 0.1	2.0 ± 0.2	8 ± 2	17 ± 5
Dimer bridge	4.1 ± 0.3	3.2 ± 0.3	17 ± 2	32 ± 2	5.0 ± 0.2	5.0 ± 0.2	39 ± 2	48 ± 2
XA3c	5.0 ± 0.1	4.8 ± 0.1	40 ± 3	49 ± 3	5.1 ± 0.1	4.7 ± 0.2	40 ± 3	49 ± 3
HELIXA4C	5.2 ± 0.3	4.3 ± 0.3	45 ± 3	59 ± 3	5.8 ± 0.3	5.4 ± 0.3	56 ± 2	65 ± 3

**Table 4** values of DNA bound and equilibrium association constants, K<sub>1</sub> and K<sub>2</sub>, reported on a logarithmic scale for the complexes between the synthesized xanthene and xanthone derivatives calculated by ESI-MS experiments

From these data, HELIXA4C seems a better G-quadruplex ligand than previously studied xanthene and xanthone derivatives<sup>11</sup>, also in the case of c-myc and bcl2 promoter sequences. This is evident also from the results of Fluorescence Resonance Energy Transfer (FRET) melting measurements, reported in Table 5. In the presence of HELIXA4C, bcl2 and c-myc show an increase of their melting temperatures respectively of 15.5 and 16.7 °C, a significantly higher increase than that caused by XA3c.

	bcl2	c-myc
XA3c	3.7 ± 0.4	3.1 ± 0.2
HELIXA4C	15.5 ± 0.9	16.7 ± 2.1

Table 5  $\Delta T_m$  data at 2  $\mu$ M ligand concentration, derived from FRET melting experiments

### Biological activity of the obtained compound HELIXA4C

Based on the results obtained *in vitro*, HELIXA4C was investigated for its antiproliferative activity against human cancer cell lines by the US National Cancer Institute (NCI). In particular, a panel of 60 human cancer cell lines derived from 9 cancer cell types (leukemia, non-small cell lung, colon, CNS, melanoma, ovarian, renal, prostate and breast) were treated for 48 h with different concentrations of HELIXA4C and the effect on cell growth was evaluated. As shown in Figure 4, the compound is effective in all the lines tested even at different extent, being the antiproliferative activity stronger in leukemia, non-small cell lung and colon cancers, with a dose-dependent behaviour.

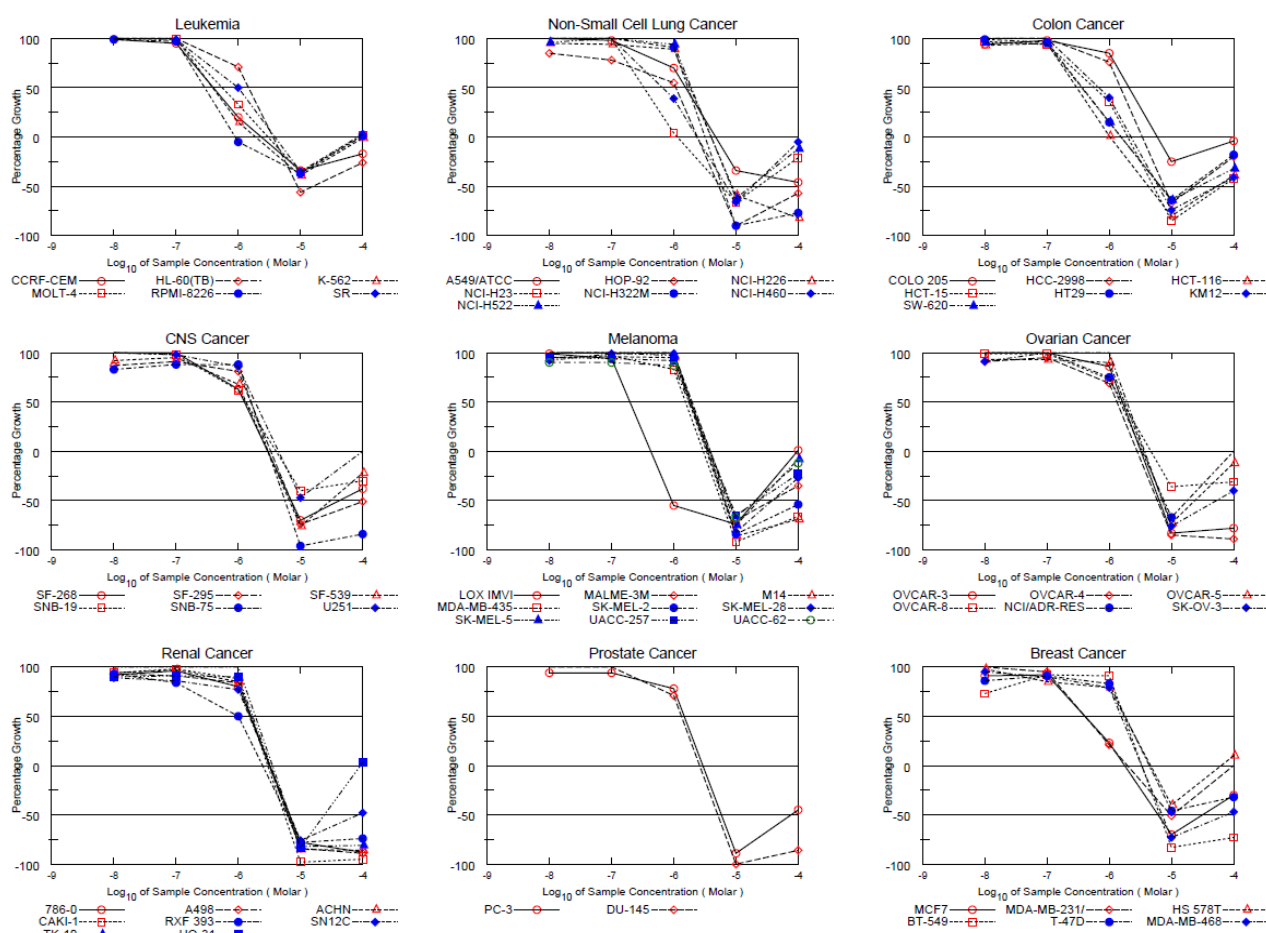
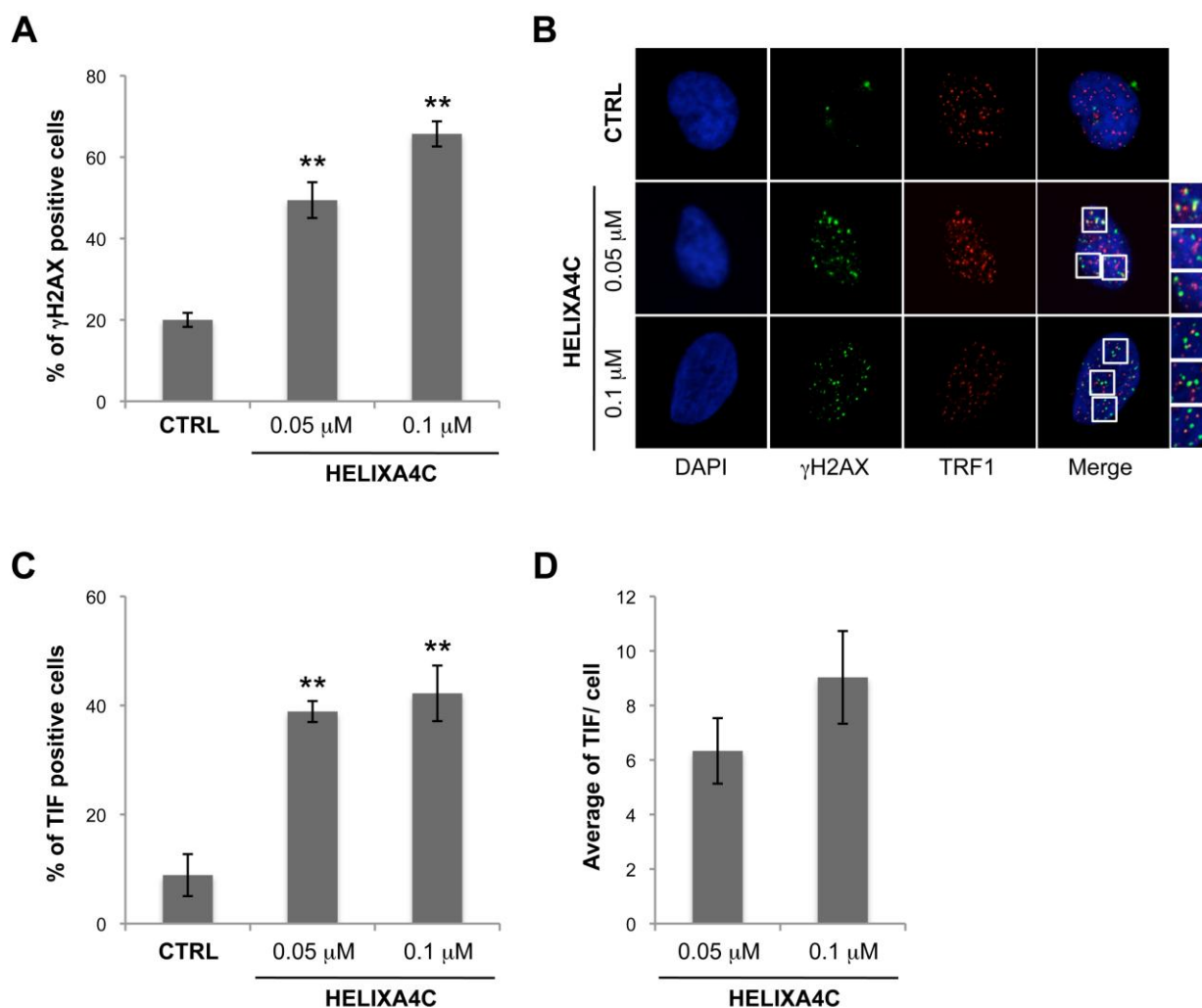


Figure 4: In Vitro Cell Line Screening 60 cell panel at five concentration levels (National Cancer Institute - NIH, Bethesda, MD, USA). Growth percent of the reported cell lines after 48 hours of incubation with the indicated concentration of HELIXA4C, with respect to no-drug control.

In light of this observation, it was then evaluated if the mechanism through which HELIXA4C exerts its antitumor activity was attributable to its capability to induce a DNA damage response (DDR). To this aim, human transformed fibroblasts (BJ-EHLT) were grown for 24hrs in absence or in presence of two different doses of HELIXA4C and the amount of phosphorylated H2AX ( $\gamma$ H2AX), a well-established hallmark of DDR<sup>38</sup>, was evaluated by immunofluorescence (IF). As shown in figure 5A, quantitative analysis of  $\gamma$ H2AX-positive cells revealed a dose-dependent activity of HELIXA4C, whose robust and highly significant effect is well appreciable at already 0.05  $\mu$ M, the lowest of the tested concentrations.

Finally, in order to define whether  $\gamma$ H2AX was phosphorylated in response to dysfunctional telomeres, double IF experiments were performed. Deconvolution microscopy showed that several of the damaged foci induced by HELIXA4C co-localized with TRF1, an effective marker for interphase telomeres, forming the so-called Telomere dysfunction Induced Foci (TIFs)<sup>39</sup> (Figure 5B), clearly indicating that the drug induced a certain amount of telomere localized damage. Consistent with these data, results from quantitative analysis revealed that HELIXA4C, at both the tested concentrations, significantly increased the percentage of cells with more than four  $\gamma$ H2AX/TRF1 co-localizations (TIF positive cells), with a mean of about 6 and 9 TIFs per nucleus, respectively (Figure 5C and D). Of note, while at the lower dose (0.05  $\mu$ M), the majority of  $\gamma$ H2AX spots localized at telomere, at the higher concentration, a certain number of the damage spots did not co-localize with TRF1. These results are perfectly in line with the above reported ESI/MS data showing that HELIXA4C, despite a strong preference for telomeric G-quadruplex structures (Table 2 and 4), maintains a moderate selectivity for certain well-documented parallel G-quadruplexes dispersed in the human genome.



**Figure 5** Analysis of DNA damage response by HELIXA4C: Transformed BJ-EHLT fibroblasts were grown in absence (CTRL) or in presence of the indicated concentrations of HELIXA4C. Upon 24 hrs, each sample was processed for IF by using antibodies against  $\gamma$ H2AX (green) and TRF1 (red) to mark DNA damage and telomeres, respectively. DAPI staining (blue) was used to mark nuclei. (A) Quantitative analysis of  $\gamma$ H2AX-positive cells. (B) Representative IF images acquired by using a Leica Deconvolution microscope (magnification 100 $\times$ ). Enlarged views of TIFs are reported on the right of each picture. (C and D) Quantification of TIF-positive cells (C) and mean of TIFs per nucleus (D) from IF experiments reported in (B). Histograms show the mean values  $\pm$ S.D. of three independent experiments. *p*-values were calculated using the *student t-test* (\*\**p* < 0.005).

## Experimental

All commercial reagents and solvents were purchased from Fluka and Sigma–Aldrich, and used without further purification. TLC glass plates (silica gel 60 F<sub>254</sub>) and silica gel 60 (0.040–0.063 mm) were purchased from Merck. Rayonet RPR-100 UV reactor. <sup>1</sup>H and <sup>13</sup>C NMR spectra were performed with Varian Mercury 300 and Bruker 400 instruments. ESI-MS spectra were recorded on a Micromass Q-TOF MICRO spectrometer. Starting compound 1 was prepared as previously described<sup>11</sup>.

### Synthesis of 3,6-Bis-(4-cloro-butoxy)-xanthen-9-one (2)

In a 50 ml flask 500mg (3,6 mmol) of compound **1** were added to 10 ml of anhydrous DMF and 4 mmol of dry Na<sub>2</sub>CO<sub>3</sub>. When the product was dissolved, it was added an excess of 1,4-dichlorobutane (0.5 ml) at room temperature and stirred for 7 hours at 70°C. Then, 10 ml of distilled water were added to the crude product and it was extracted three times with 30 ml of DCM. The organic phase were washed with 10 ml of NaCl saturated aqueous solution for three times and finally dried with Na<sub>2</sub>SO<sub>4</sub>. The product was purified by crystallization in hexane, obtaining **2** as a white solid (650 mg, 1.64 mmol, 73% yield). <sup>1</sup>H NMR (300MHz), CDCl<sub>3</sub>; δ 8,20 (2H, d, aromatic), δ 6,88 (2H, d, aromatic); δ 6.80 (2H, d, aromatic); δ 4.09 (4H, m, -CH<sub>2</sub>-O); δ 3.64 (4H, d, -CH<sub>2</sub>Cl); δ 2.00 (8H, m, -CH<sub>2</sub>-). <sup>13</sup>C NMR (75MHz), CDCl<sub>3</sub>; δ 175.5 (Ph-(CO)Ph); δ 164.0, 158.0, 128.20, 115.9, 113.2, 100.8 (aromatic); δ 67.7 (-CH<sub>2</sub>O-); δ 29.3, 26.5 (-CH<sub>2</sub>-); δ 29.98 (-CH<sub>2</sub>Cl). HRMS *m/z* calc. C<sub>21</sub>H<sub>22</sub>Cl<sub>2</sub>O<sub>4</sub> [M+Na]<sup>+</sup>.432.3028, found [M+Na]<sup>+</sup>432.3024

### Synthesis of 3,6,3',6'-Tetrakis-(4-chloro-butoxy)-[9,9']bixanthenylidene (**3**)

In a glass tube with screw cap anhydrous AlCl<sub>3</sub> (99 mg, 0.74 mmol) and Zn metal (48.4 mg, 0.74 mmol) in 3 ml of anhydrous THF were mixed, then 150 mg (0.37 mmol) of compound **2** were added under argon. The mixture was heated in a microwave oven (CEM Mars 5) at 60 °C for 10 min using an effective power of 12 W. After completion of the reaction (controlled by TLC 20% CHCl<sub>3</sub> in hexane), distilled water was added to the reaction mixture and the precipitate was filtered and washed with distilled water, obtaining 118.3 mg (0.15 mmol) of compound **3** as a yellow solid (81% yield). <sup>1</sup>H NMR (300MHz), CDCl<sub>3</sub>; δ 7.08 (4H, d, aromatic), δ 6,74 (4H, s, aromatic); δ 6.47 (4H, d, aromatic); δ 4.00 (8H, m, -CH<sub>2</sub>-O); δ 3.63 (8H, m, -CH<sub>2</sub>Cl); δ 1.97 (16H, m, -CH<sub>2</sub>-). <sup>13</sup>C NMR (75MHz), CDCl<sub>3</sub>; δ 158.8, 156.6, 128.8, 118.7, 118.3, 110.0 (aromatic); δ 67.3 (-CH<sub>2</sub>O-); δ 44.9, 29.4 (-CH<sub>2</sub>-); δ 26.7 (-CH<sub>2</sub>Cl). HRMS *m/z* calc. C<sub>42</sub>H<sub>44</sub>Cl<sub>4</sub>O<sub>6</sub> [M+Na]<sup>+</sup> 809.6145, found [M+Na]<sup>+</sup> 809.6139

### Synthesis of 2,5,9,14-Tetrakis-(4-chloro-butoxy)-7,16-dioxa-dibenzo[a,o]perylene (**4**)

In a 40 ml quartz tube 100 mg (0.127 mmol) of compound **3** and 150 mg of I<sub>2</sub> were added in 30 ml of anhydrous THF under argon. The tube was sealed and irradiated for 14 h in a UV reactor (Rayonet photochemical reactor RPR - 100). After completion of the reaction (controlled by TLC 20% CHCl<sub>3</sub> in hexane), the solution was extracted in CHCl<sub>3</sub>, then washed with a saturated solution of sodium thiosulfate, distilled water and finally with a saturated solution of NaCl. The organic phase was then dried with anhydrous sodium sulphate, filtered and taken to dryness in vacuum. The crude product was purified by chromatography (0%-40% CHCl<sub>3</sub> in hexane). 80 mg (0.10 mmol) of **4** were obtained as a yellow-green oil (80% yield). <sup>1</sup>H NMR (300MHz), DMSO; δ 7.68 (2H, d, aromatic), δ 6,52 (2H, s, aromatic); δ 6.79 (2H, s, aromatic); δ 6.71 (2H, s, aromatic); δ 6.56 (2H, d, aromatic); δ 4.18 (4H, m, -CH<sub>2</sub>-O); δ 4.04 (4H, m, -CH<sub>2</sub>-O); δ 3.72 (8H, m, -CH<sub>2</sub>Cl); δ 1.91, 1.88 (16H, m, -CH<sub>2</sub>-). <sup>13</sup>C NMR (75MHz), DMSO; δ 159.5, 157.8, 153.0, 151.2, 129.4, 127.5, 116.1, 113.7, 113.5, 110.5 101.7, 101.2, 101.1(aromatic); δ 67.1 (-CH<sub>2</sub>O-); δ 45.1, 45.0, 28.9, 28.8, 26.1 26.0 (-CH<sub>2</sub>-). HRMS *m/z* calc. C<sub>42</sub>H<sub>42</sub>Cl<sub>4</sub>O<sub>6</sub> [M+Na]<sup>+</sup> 807.6143, found [M+Na]<sup>+</sup>807.6147

### Synthesis of 2,5,9,14-Tetrakis-(4-piperidino-butoxy)-7,16-dioxa-dibenzo[a,o]perylene (**5**, HELIXA4C)

80 mg (0.10 mmol) of compound **4** were dissolved in ACN dry (5 ml) and treated with an excess of the piperidine (8 eq) in an ice bath, then stirred at reflux for 4 hours. After completion of the reaction (controlled by TLC 20% MeOH in DCM), solvent was evaporated in vacuum. The crude product was dissolved in DCM (75 ml), washed 3 times with brine (50 ml), dried over Na<sub>2</sub>SO<sub>4</sub>, filtered and taken to dryness in vacuum. The crude product was purified by chromatography column (5%-40% MeOH in DCM), obtaining 61 mg of **5** (HELIXA4C, 0.06 mmol, 60% yield). <sup>1</sup>H NMR (300 MHz), DMSO, δ 7.71 (2H, d,aromatic); δ 7.60 (2H, s, aromatic); δ 6.85 (2H, s, aromatic); δ 6.76 (2H, s,aromatic); δ 6.59 (2H, d,aromatic);δ 3.75

(4H, m CH benzylic);  $\delta$  3.50 (4H, m -CH<sub>2</sub>-);  $\delta$  2.22 (8H, m -CH<sub>2</sub>-);  $\delta$  1.78 – 1.24 (40H, m, -CH<sub>2</sub>-). <sup>13</sup>C NMR (100MHz), MeOD:  $\delta$  159.5, 157.8, 153.0, 151.2, 129.4, 127.5, 116.1, 113.7, 113.5, 110.5, 101.7, 101.2, 101.1 (aromatic); 67.2, 67.0 (-OCH<sub>2</sub>-), 55.9, 52.54 (-CH<sub>2</sub>N-), 26.4, 26.2, 23.0, 21.7, 20.8, 20.7, 20.5 (-CH<sub>2</sub>-). HRMS *m/z* calc. C<sub>62</sub>H<sub>82</sub>N<sub>4</sub>O<sub>6</sub> [M+H]<sup>+</sup> 979.0322, found [M+H]<sup>+</sup> 979.0324. Molecular Composition: C 67.3% H 7.8% Cl 9.6% N 5.0% O 10.0% corresponding to C<sub>62</sub>H<sub>82</sub>N<sub>4</sub>O<sub>6</sub> · 3HCl · H<sub>2</sub>O.

### Molecular Modelling - Docking calculation

The crystal structure used was that of the parallel 22-mer telomeric G-quadruplex (PDB ID: 1KF1) Ligand structures were constructed by adopting Avogadro1.0.3 for force field optimization by using the MMFF94 steepest descent algorithm. Docking studies were performed with the AUTODOCK 4.2 program. Water molecules were removed from the PDB file, nonpolar hydrogen atom of the telomeric G-quadruplex were added to their corresponding carbon atoms, and partial atomic charges were assigned, by using ADT. The Lamarckian genetic algorithm (LGA) was used to perform docking calculations. A population of random individuals was initially used (population size: 150), with a maximum number of 25,000,000 energy evaluations, a maximum number of generations of 27,000, and a mutation rate of 0.02. 100 independent docking runs were carried out for each ligand. The resulting positions were clustered according to a root-mean-square criterion of 0.5 Å. Docking module was used to calculate the intermolecular (binding) energy, obtained as a sum of electrostatic and van der Waals contributions, between ligand and DNA. The corresponding intermolecular energy values were used to calculate the average binding energies and the relative standard deviations.

### Analysis of the DNA-Drug Interactions by ESI-MS

*Instrumentation:* All the experiments were performed on a Q-TOF MICRO spectrometer (Micromass, now Waters, Manchester, UK) equipped with an ESI source, in the negative ionization mode. The rate of sample infusion into the mass spectrometer was 5 or 10  $\mu$ L/min and the capillary voltage was set to -2.6 kV. The source temperature was adjusted to 70 °C and the source pressure was set at 1.30 mbar. The cone voltage was set to 30 V and the collision energy to 10 V. Full scan MS spectra were recorded in the *m/z* range between 800 and 2,500, with 100 acquisitions per spectrum. Data were analyzed using the MassLynx software developed by Waters.

*Sample preparation protocol:* Oligonucleotides were dissolved in bi-distilled water to obtain the starting stock solutions and were annealed in 150 mM ammonium acetate buffer by heating at 90 °C for 10 min and then cooling slowly to room temperature. The final concentration of oligonucleotides stocks was 50  $\mu$ M in either duplex or quadruplex units. Ammonium acetate was chosen as the buffer main component for its good compatibility with ESI-MS. Calf thymus DNA (CT) was dissolved in bi-distilled water. Since its average chain length is 13 kb, it was subjected to sonication (Sonymprep 150 sonicator) for 8 min to obtain an average length of 500 bp (according to gel electrophoresis analysis with Mass Ruler DNA ladder mix-low range). Drug stock solutions were prepared by dissolving in bi-distilled water the desired amount of drug hydrochlorides to obtain a final concentration of 100  $\mu$ M.

Samples were prepared by mixing appropriate volumes of 150 mM ammonium acetate buffer, 50  $\mu$ M annealed oligonucleotide stock solution, xanthene or xanthone derivatives 100  $\mu$ M stock solutions and methanol<sup>40</sup>. The final concentration of DNA in each sample was 5  $\mu$ M (in duplex or quadruplex unit) and the final volume of the sample was 50  $\mu$ L. Drugs were added at different drug/DNA ratios, ranging between 0.5 and 4. Methanol was added to the mixture just before injection (in a percentage of 15% vol.) after the

complexation equilibrium in ammonium acetate was established, in order to obtain a stable electrospray signal. As a reference, samples containing only 5  $\mu\text{M}$  DNA with no drug were prepared in each series.

Samples for competition experiments were prepared following the procedure described above, adding an appropriate volume of CT solution. Final concentrations of quadruplex DNA and drug solutions were always 5  $\mu\text{M}$  and CT was added at two different duplex/quadruplex ratios (1 and 5), calculated on the basis of the phosphate group concentrations. In order to minimize casual errors each experiment has been repeated at least three times, in the same experimental conditions, and data were processed and averaged with the SIGMA-PLOT software.

Binding constants ( $K_1$  and  $K_2$ ) and percentage of bound DNA have been calculated according to previously reported formulae<sup>38</sup>. Considering drug-DNA complexes in 1:1 and 2:1 stoichiometry, which have been proven to be the main species present in solution in all the experiments, the formation of such complexes can be represented by two distinct equilibria:

DNA + drug 1:1

drug + 1:1 2:1

which are in turn described by the following two equations:

$$K_1 = [1:1]/([DNA][drug]) \quad (1)$$

$$K_2 = [2:1]/([1:1][drug]) \quad (2)$$

where [DNA], [drug], [1:1] and [2:1] represent respectively the concentrations of the different species in solution: DNA (duplex or quadruplex depending on the oligonucleotide used), the ligand, the 1:1 and 2:1 drug-DNA complexes at equilibrium. The association constants  $K_1$  and  $K_2$  (Equations (1) and (2), respectively) can be calculated directly from the relative intensities of the corresponding peaks found in the mass spectra, with the assumption that the response factors of the oligonucleotides alone and of the drug-DNA complexes are the same, so that the relative intensities in the spectrum are proportional to the relative concentrations in the injected solution:

$$[DNA]/[DNA] = I(1:1)/[1:1] = I(2:1)/[2:1] \quad (3)$$

In this way, since DNA and drugs initial concentrations ( $C_0$  and  $C_0'$  respectively) are known, it is possible to obtain the concentration of each species appearing in 1 and 2:

$$[j] = C_0 \cdot I(j)/(I(DNA) + I(1:1) + I(2:1)) \quad (4)$$

$$[drug] = C_0' - [1:1] - 2[2:1] \quad (5)$$

where [j] stands for [DNA], [1:1] or [2:1].

The constants were determined at different drug/DNA ratios, depending on the intensity of the signals 2.5:5, 5:5, 7.5:5, 10:5 and 20:5 micromolar concentrations ratios. A further manipulation of the data leads to the calculation of the amount of ligand bound, according to an equation developed by de Pauw and his group [24] derived from Equation (4):

$$[\text{ligand bound}] = C_0 (I(1:1) + 2I(2:1))/(I(DNA) + I(1:1) + I(2:1)) \quad (6)$$

This parameter, representing the total amount of the drug bound to DNA, is useful to compare the efficiency of different ligands in DNA binding, when they interact as single molecules. Since planar aromatic derivatives are known to also interact with DNA in self-aggregate forms, we decided to use:

$$\%_{\text{bound DNA}} (\%_b) = 100 \cdot (I(1:1) + I(2:1)) / (I(\text{DNA}) + I(1:1) + I(2:1)) \quad (7)$$

This parameter ( $\%_b$ ) represents the percentage of DNA bound to the ligand.

## G-quadruplex melting assays

### Fluorescence Resonance Energy Transfer (FRET)

*Instrumentation:* Measurements were made on an iCycler thermal cycler (Bio-Rad Laboratories, Hercules, CA) with excitation at 450–495 nm and detection at 515–545 nm. Fluorescence readings were taken at intervals of 0.2°C over the range 25–95°C, with a constant temperature being maintained for 12 seconds prior to each reading. All melting temperature experiments were carried out in triplicate. The melting temperature ( $T_m$ ) was deduced as the temperature corresponding to 50% of the folded fraction.

*Sample preparation protocol:* The labeled oligonucleotides used as the FRET probe (F-myc-T, 5'-FAM-GAGGGTGGGGAGGGTGGGGAA-TAMRA-3', and F-bcl2-T, 5'-FAM-GGGCGCGGGAGGAAGGGGGCGGG-TAMRA-3'; donor fluorophore FAM: 6-carboxyfluorescein; acceptor fluorophore TAMRA: 6-carboxy-tetramethylrhodamine) were diluted from stock to the correct concentration (800 nM) in a 0.5 mM potassium cacodylate buffer (pH 7.4) with 100 mM LiCl and then annealed by heating to 85 °C for 10 min, followed by cooling to room temperature in the heating block. Relevant controls were also performed to ascertain a lack of interference with the assay (not shown). 96-well plates (Aurogene, Rome, IT) were prepared by aliquoting 25  $\mu$ l of the annealed DNA to each well, followed by 25  $\mu$ l of the compound solutions.

### Circular Dichroism (CD) spectroscopy

*Instrumentation:* CD spectra were recorded on a JASCO J-715 spectropolarimeter equipped with a Peltier temperature controller, using a quartz cell of 0.5 cm optical path length. The CD melting curves of HTelo21 oligonucleotide (5'-GGGTTAGGGTTAGGGTTAGGG-3') were obtained by recording the ellipticity corresponding to the CD spectra maximum at 292 nm as a function of temperature, at intervals of 1°C over the range 25–95°C. The resulting CD melting profiles were normalized obtaining a plot of the folded fraction,  $\alpha$ , versus temperature. The melting temperature ( $T_m$ ) was then deduced as the temperature corresponding to  $\alpha$  equal to 0.5.

*Sample preparation protocol:* HTelo21 oligonucleotide were diluted to 2.5  $\mu$ M concentration in TE buffer (Tris-HCl 10 mM pH 7.6, and EDTA 1 mM) and 50 mM KCl, then annealed by heating at 95°C for 10 minutes and then slow cooling to room temperature in the heating block. The CD melting profile was recorded for HTelo21 alone or in the presence of HELIXA4C, at the concentration of 12.5  $\mu$ M, in order to achieve a drug/DNA ratio equal to 5.

## Methodology Of The In Vitro Cancer Screen

The human tumor cell lines of the cancer screening panel are grown in RPMI 1640 medium containing 5% fetal bovine serum and 2 mM L-glutamine. For a typical screening experiment, cells are inoculated into 96 well microtiter plates in 100  $\mu$ L at plating densities ranging from 5,000 to 40,000 cells/well depending on the doubling time of individual cell lines. After cell inoculation, the microtiter plates are incubated at 37° C, 5 % CO<sub>2</sub>, 95 % air and 100 % relative humidity for 24 h prior to addition of experimental drugs.

After 24 h, two plates of each cell line are fixed *in situ* with TCA, to represent a measurement of the cell population for each cell line at the time of drug addition (T<sub>z</sub>). Experimental drugs are solubilized in dimethyl sulfoxide at 400-fold the desired final maximum test concentration and stored frozen prior to use. At the time of drug addition, an aliquot of frozen concentrate is thawed and diluted to twice the desired final maximum test concentration with complete medium containing 50  $\mu$ g/ml gentamicin. Additional four, 10-fold or ½ log serial dilutions are made to provide a total of five drug concentrations plus control. Aliquots of 100  $\mu$ L of these different drug dilutions are added to the appropriate microtiter wells already containing 100  $\mu$ L of medium, resulting in the required final drug concentrations.

Following drug addition, the plates are incubated for an additional 48 h at 37°C, 5 % CO<sub>2</sub>, 95 % air, and 100 % relative humidity. For adherent cells, the assay is terminated by the addition of cold TCA. Cells are fixed *in situ* by the gentle addition of 50  $\mu$ L of cold 50 % (w/v) TCA (final concentration, 10 % TCA) and incubated for 60 minutes at 4°C. The supernatant is discarded, and the plates are washed five times with tap water and air dried. Sulforhodamine B (SRB) solution (100  $\mu$ L) at 0.4 % (w/v) in 1 % acetic acid is added to each well, and plates are incubated for 10 minutes at room temperature. After staining, unbound dye is removed by washing five times with 1 % acetic acid and the plates are air dried. Bound stain is subsequently solubilized with 10 mM trizma base, and the absorbance is read on an automated plate reader at a wavelength of 515 nm. For suspension cells, the methodology is the same except that the assay is terminated by fixing settled cells at the bottom of the wells by gently adding 50  $\mu$ L of 80 % TCA (final concentration, 16 % TCA). Using the seven absorbance measurements [time zero, (T<sub>z</sub>), control growth, (C), and test growth in the presence of drug at the five concentration levels (T<sub>i</sub>)], the percentage growth is calculated at each of the drug concentrations levels. Percentage growth inhibition is calculated as:

$$[(T_i - T_z) / (C - T_z)] \times 100 \text{ for concentrations for which } T_i \geq T_z$$

$$[(T_i - T_z) / T_z] \times 100 \text{ for concentrations for which } T_i < T_z.$$

Three dose response parameters are calculated for each experimental agent. Growth inhibition of 50 % (GI<sub>50</sub>) is calculated from  $[(T_i - T_z) / (C - T_z)] \times 100 = 50$ , which is the drug concentration resulting in a 50% reduction in the net protein increase (as measured by SRB staining) in control cells during the drug incubation. The drug concentration resulting in total growth inhibition (TGI) is calculated from  $T_i = T_z$ . The LC<sub>50</sub> (concentration of drug resulting in a 50% reduction in the measured protein at the end of the drug treatment as compared to that at the beginning) indicating a net loss of cells following treatment is calculated from  $[(T_i - T_z) / T_z] \times 100 = -50$ . Values are calculated for each of these three parameters if the level of activity is reached; however, if the effect is not reached or is exceeded, the value for that parameter is expressed as greater or less than the maximum or minimum concentration tested.

## Immunofluorescence

Immunofluorescence (IF) was performed as previously described<sup>6</sup> in BJ-EHLT fibroblasts, expressing hTERT plus SV40 early region. Briefly, cells were fixed in 2% formaldehyde and permeabilized in PBS plus 0.25% Triton X-100 for 5 min at room temperature. For immunolabeling, cells were incubated with primary antibody for two hrs at room temperature, washed twice in PBS and finally incubated with the secondary antibodies for 1 hr. The following antibodies were used: rabbit polyclonal anti-TRF1 antibody (Abcam Ltd.; Cambridge UK); mouse monoclonal anti- $\gamma$ H2AX antibody (Upstate, Lake Placid, NY); TRITC-conjugated Goat anti-Rabbit, FITC-conjugated Goat anti Mouse (Jackson ImmunoResearch, Suffolk, UK.). Nuclei were immunostained with DAPI. Fluorescence signals were recorded by using a Leica DMIRE2 microscope equipped with a Leica DFC 350FX camera and elaborated by Leica FW4000 deconvolution software (Leica, Solms, Germany). For quantitative analysis of  $\gamma$ H2AX positivity, 200 cells on triplicate slices were scored. For TIF analysis, a single plane was analyzed and 30  $\gamma$ H2AX-positive cells were scored. Cells with at least 4 co-localizations ( $\gamma$ H2AX /TRF1) were considered as TIF-positive.

The experiments have been repeated three times and the obtained results are presented as means  $\pm$  standard deviation (S.D.). Significant changes were assessed by using Student's t test for unpaired data, and  $p$  values  $<0.05$  (\*) were considered significant.

## Conclusion

Here we reported the synthesis and the characterization of a new dimeric xanthone derivative, where the extension of the aromatic core and the increasing of the number of polar side chains led to great enhancement of G-quadruplex selectivity and telomere damage capability. Indeed, the initial design suggested a good interaction with quadruplex DNA, despite the molecule is not fully planar. We succeeded in the synthesis of the designed compound, using a variant of the McMurry reaction. ESI-MS evaluation, including competitive experiments, showed association constants higher than those obtained for the previously reported xanthene and xanthone derivatives<sup>11</sup>, comparable with the best ligands tested to date among those we prepared in our group so far, CORON and EMICORON<sup>41,42</sup>. The selectivity for G-quadruplex with respect to duplex DNA and the ability to bind different G-quadruplex forming sequences, specifically related to G-rich oncogenes promoter sequences, have also been shown to be good for the new compound HELIXA4C. Based on the results obtained *in vitro*, HELIXA4C was investigated for its antiproliferative activity against human cancer cell lines by the US National Cancer Institute (NCI), showing a good activity in all the lines tested even at different extent, being the antiproliferative activity stronger in leukemia, non-small cell lung and colon cancers, with a dose-dependent behaviour. Finally, it was evaluated if the mechanism through which HELIXA4C exerts its antitumor activity was attributable to its capability induce a DNA damage response. However, even if the experimental results clearly indicated that the drug induces a certain amount of telomere-localized damage, the molecular mechanism through which the ligand disrupts telomere function and causes cell growth arrest needs to be fully elucidated<sup>43,44</sup>. Therefore, the new compound HELIXA4C deserves further investigation as promising anticancer agent.

## Acknowledgements

This work has been financially supported by Ministero dell'Istruzione, dell'Università e della Ricerca (MIUR, PRIN 2009) and by Università di Roma "La Sapienza" and from the Italian Association for Cancer Research

(A.I.R.C., # 11567). C.C. is recipient of a fellowship from the Italian Foundation for Cancer Research (F.I.R.C.).

## Bibliographic references

1. Ohnmacht, S.A.; Ciancimino, C.; Vignaroli, G.; Gunaratnam, M.; Neidle, S.; Optimization of anti-proliferative activity using a screening approach with a series of bis-heterocyclic G-quadruplex ligands., *Bioorg & Med. Chem. Lett.* 2013, 23 5351 - 5355.
2. Zahler, A. M., Williamson, J. R., Cech, T. R. & Prescott, D. M. Inhibition of telomerase by G-quartet DMA structures. *Nature*.1991, 350, 718–720.
3. Rodriguez, R., Pantos, G. D., Goncalves, D. P. N., Sanders, J. K. M. Balasubramanian, S. Ligand-driven G-quadruplex conformational switching by using an unusual mode of interaction. *Angew. Chem. Int. Ed.* 46, 5405–5407 (2007).
4. Sun, D.; Thompson, B.; Cathers, B. E.; Salazar, M.; Kerwin, S. M.; Trent, J. O.; Jenkins, T. C.; Neidle, S.; Hurley, L. H. Inhibition of human telomerase by a G-quadruplex-interactive compound. *J. Med. Chem.* 1997, 40, 2113–2116.
5. Biffi, G.; Tannahill, D.; McCafferty, J.; Balasubramanian, S. Quantitative visualization of DNA G-quadruplex structures in human cells. *Nature Chem.* 2013, 5, 182–186.
6. Salvati, E.; Leonetti, C.; Rizzo, A.; Scarsella, M.; Mottolese, M.; Galati, R.; Sperduti, I.; Stevens, M. F.; D'Incalci, M.; Blasco, M.; Chiorino, G.; Bauwens, S.; Horard, B.; Gilson, E.; Stoppacciaro, A.; Zupi, G.; Biroccio, A. Telomere damage induced by the G-quadruplex ligand RHPS4 has an antitumor effect. *J. Clin. Invest.* 2007, 117, 3236–3247.
7. Adams, J.M.; Cory, S. The Bcl-2 apoptotic switch in cancer development and therapy. *Oncogene*, 2007, 26, 1324–1337.
8. Rangan, A.; Fedoroff, O. Y.; Hurley, L. H. Induction of duplex to G-quadruplex transition in the c-myc promoter region by a small molecule. *J. Biol. Chem.* 2001, 276, 4640- 4646.
9. Seenisamy, J.; Rezler, E. M.; Powell, T. J.; Tye, D.; Gokhale, V.; Joshi, C. S.; Siddiqui-Jain, A. Hurley, L. H. The dynamic character of the G-quadruplex element in the cmyc promoter and modification by TMPyP4. *J. Am. Chem. Soc.* 2004, 126, 8702- 8709.
10. Franceschin, M. G-quadruplex DNA structures and organic chemistry: More than one connection. *Eur. J. Org. Chem.* 2009, 2009, 2225–2238.
11. Altieri, A., Alvino, A., Ohnmacht, S., Ortaggi, G., Neidle, S., Nocioni, D., Franceschin, M., Bianco, M., Xanthene and Xanthone Derivatives as G-Quadruplex Stabilizing Ligands, *Molecules* 2013, 18, 13446-13470.
12. Franceschin M., Alvino A., Casagrande V., Mauriello C., Pascucci E., Savino M., Ortaggi G., Bianco A. "Specific interactions with intra- and intermolecular G-quadruplex DNA structures by hydrosoluble coronene derivatives: a new class of telomerase inhibitors" *Bioorg. Med. Chem.* 2007, 15, 1848-1858.
13. John E. McMurry, Michael P. Fleming "New method for the reductive coupling of carbonyls to olefins. Synthesis of  $\beta$ -carotene". *J. Am. Chem. Soc.* 1974, 96 (14): 4708–4709.
14. Ian C. Richards "Titanium(IV) Chloride–Zinc" in *Encyclopedia of Reagents for Organic Synthesis*, John Wiley, London, 2001
15. Martin G. Banwell, "Titanium(III) Chloride–Lithium Aluminum Hydride" in *Encyclopedia of Reagents for Organic Synthesis* John Wiley, London, 2001
16. Neo AG, López C, Romero V, Antelo B, Delamano J, Pérez A, Fernández D, Almeida JF, Castedo L, Tojo G. Preparation of phenanthrenes by photocyclization of stilbenes containing a tosyl group on the central double bond. A versatile approach to the synthesis of phenanthrenes and phenanthrenoids. *J Org Chem.* 2010 Oct 15;75(20):6764-70.
17. Mao M, Wu QQ, Ren MG, Song QH. Highly efficient and regiospecific photocyclization of 2,2'-diacyl bixanthylenes. *Org Biomol Chem.* 2011 May 7;9(9):3165-9.
18. Mallory, F.B.; Mallory, C.W. Photocyclization of stilbenes and related molecules. *Org. React.* 1984, 30.
19. Kåre B. Jørgensen, Photochemical Oxidative Cyclisation of Stilbenes and Stilbenoids—The Mallory-Reaction *Molecules* 2010, 15, 4334-4358.
20. Morris, G.M.; Huey, R.; Lindstrom, W.; Sanner, M.F.; Belew, R.K.; Goodsell, D.S.; Olson, A.J. AutoDock4 and AutoDockTools4: Automated docking with selective receptor flexibility. *J. Comput. Chem.* 2009, 30, 2785–2791.
21. Cosconati, S.; Marinelli, L.; Trotta, R.; Virno, A.; Mayol, L.; Novellino, E.; Olson, A.J.; Randazzo, A. Tandem application of virtual screening and NMR experiments in the discovery of brand new DNA quadruplex groove binders. *J. Am. Chem. Soc.* 2009, 131, 16336–16337.

22. Lane, A.N.; Chaires, J.B.; Gray, R.D.; Trent, J.O. Stability and kinetics of G-quadruplex structures. *Nucleic Acids Res.*, 2008, 36, 5482–5515
23. Parkinson, G.N.; Lee, M.P.; Neidle, S. Crystal structure of parallel quadruplexes from human telomeric DNA. *Nature* 2002, 417, 876–880.
24. Husby, J.; Todd, A.K.; Platts, J.A.; Neidle, S. Small-molecule G-quadruplex interactions: Systematic exploration of conformational space using multiple molecular dynamics. *Biopolymers* 2013, 99, 989–1005.
25. Franceschin, M.; Pascucci, E.; Alvino, A.; D'Ambrosio, D.; Bianco, A.; Ortaggi, G.; Savino, M. New highly hydrosoluble and not self-aggregated perylene derivatives with three and four polar side chains as G-quadruplex telomere targeting agents and telomerase inhibitors. *Bioorg. Med. Chem. Lett.* 2007, 17, 2515–2522.
26. Franceschin, M.; Casagrande, V.; Salvati, E.; Alvino, A.; Bianco, A.; Altieri, A.; Ciammaichella, A.; D'Angelo, C.; Iachettini, S.; Leonetti, S.; Neidle, S.; Porru, M.; Rizzo, A.; Biroccio, A.; Aromatic Core Extension in the Series of N-Cyclic Bay-Substituted Perylene G-Quadruplex Ligands: Increased Telomere Damage, Antitumor Activity, and Strong Selectivity for Neoplastic over Healthy Cells, *ChemMedChem* 2012, 7, 2144 - 2154.
27. Casagrande, V.; Alvino, A.; Bianco, A.; Ortaggi, G.; Franceschin, M. Study of binding affinity and selectivity of perylene and coronene derivatives towards duplex and quadruplex DNA by ESI-MS. *J. Mass Spectrom.* 2009, 4, 530–540.
28. Altieri, A.; Franceschin, M.; Nocioni, D.; Alvino, A.; Casagrande, V.; Scarpati, M.L.; Bianco, A. Total synthesis of taspine and a symmetrical analogue: Study of binding to G-quadruplex DNA by ESI-MS. *Eur. J. Org. Chem.*, 2013, 191–196.
29. Gabelica, V.; de Pauw, E.; Rosu, F. Interaction between antitumor drugs and a double-stranded oligonucleotide studied by electrospray ionization mass spectrometry. *J. Mass Spectrom.* 1999, 34, 1328–1337.
30. Gabelica, V.; Rosu, F.; Houssier, C.; de Pauw, E. Gas phase thermal denaturation of an oligonucleotide duplex and its complexes with minor groove binders. *Rapid Comm. Mass Spectrom.* 2000, 14, 464–467.
31. Franceschin, M.; Alvino, A.; Ortaggi, G.; Bianco, A. New hydrosoluble perylene and coronene derivatives. *Tetrahedron Lett.* 2004, 45, 9015–9020.
32. Casagrande, V.; Salvati, E.; Alvino, A.; Bianco, A.; Ciammaichella, A.; D'Angelo, C.; Iachettini, S.; Leonetti, S.; Neidle, S.; Porru, M.; Rizzo, A.; Franceschin, M.; Biroccio, A. N-Cyclic Bay-Substituted Perylene G-Quadruplex Ligands Have Selective Antiproliferative Effects on Cancer Cells and Induce Telomere Damage *J. Med. Chem.* 2011, 54, 1140–1156.
33. Yu H, Wang X, Fu M, Ren J, Qu X Chiral metallo-supramolecular complexes selectively recognize human telomeric G-quadruplex DNA, *Nucleic Acids Res.* 2008,36, 5695-703
34. Zhao C., Wu L., Ren J., Xu Y., Qu X. Targeting human telomeric higher-order DNA: dimeric G-quadruplex units serve as preferred binding site. *J. Am. Chem. Soc.* 2013;135, 18786-18789.
35. Casagrande, V.; Alvino, A.; Bianco, A.; Ortaggi, G.; Franceschin, M. Study of binding affinity and selectivity of perylene and coronene derivatives towards duplex and quadruplex DNA by ESI-MS. *J. Mass. Spectrom.* 2009, 4, 530–540.
36. Mathad, R.; Hatzakis, E.; Dai, X.; Yang, D.; c-MYC promoter G-quadruplex formed at the 50-end of NHE III1 element: insights into biological relevance and parallel-stranded G-quadruplex stability - *Nucleic Acids Research*, 2011, 39, 9023–9033
37. Dexheimer, T.S., Sun, D., and Hurley, L.H. (2006). Deconvoluting the structural and drug-recognition complexity of the G-quadruplex-forming region upstream of the bcl-2 P1 promoter. *J Am Chem Soc* 128, 5404-5415.
38. Thiriet, C.; Hayes, J.J. Chromatin in need of a fix: phosphorylation of H2AX connects chromatin to DNA repair - *Mol. Cell.* 2005, 18, 617-622
39. Takai, H.; Smogorzewska, A.; de Lange T. DNA damage foci at dysfunctional telomeres - *Curr. Biol.* 2003, 13, 1549-1556.
40. Altieri, A.; Franceschin, M.; Nocioni, D.; Alvino, A.; Casagrande, V.; Scarpati, M.L.; Bianco, A. Total synthesis of taspine and a symmetrical analogue: Study of binding to G-quadruplex DNA by ESI-MS. *Eur. J. Org. Chem.* 2013, 2013, 191–196.
41. Franceschin, M.; Alvino, A.; Ortaggi, G.; Bianco, A. New hydrosoluble perylene and coronene derivatives. *Tetrahedron Lett.* 2004, 45, 9015–9020.
42. Casagrande, V.; Salvati, E.; Alvino, A.; Bianco, A.; Ciammaichella, A.; D'Angelo, C.; Iachettini, S.; Leonetti, S.; Neidle, S.; Porru, M.; Rizzo, A.; Franceschin, M.; Biroccio, A. N-Cyclic Bay-Substituted Perylene G-Quadruplex Ligands Have Selective Antiproliferative Effects on Cancer Cells and Induce Telomere Damage *J. Med. Chem.* 2011, 54, 1140–1156.
43. Wang, J., Chen, Y., Ren, J., Zhao, C., Qu, X. G-Quadruplex binding enantiomers show chiral selective interactions with human telomere. *Nucleic Acids Res.* 2014, 6, 3792-3802.

44. Chen, Y., Qu, K., Zhao, C., Wu, L., Ren, J., wang, J., Qu, X. Insights into the biomedical effects of carboxylated single-wall carbon nanotubes on telomerase and telomeres. *Nat Commun.* 2012, 3, 1074-1087.